A Special Refereed Issue (Volume 19) – Selected articles from the International Engineering Technologies and Applied Sciences Conference and Exhibition, Baghdad, Iraq, 2024

https://doi.org/10.14525/JJCE.v19i5.05

Jordan Journal of Civil Engineering

Journal homepage: https://jjce.just.edu.jo

Lateral Dynamic Pressures on Retaining Wall Adjacent to Railway Track

Kather A. Naji [1)*], Mohammed A. Al- Neami [2)], and Mahmood R. Mahmood [3)]

[1)] *PhD Student, Civil Engineering Department, University of Technology, Iraq.*
* *Corresponding Author. Email: bce.20.37@grad.uotechnology.edu.iq*
[2)] *Professor, Civil Engineering Department, University of Technology, Iraq. Email: 40008@uotechnology.edu.iq*
[3)] *Professor, Civil Engineering Department, University of Technology, Iraq. Email: 40079@uotechnology.edu.iq*

Pages: 44 - 52

Published: August, 2025

ABSTRACT

Due to the limited number of experimental laboratory studies examining the effects of dynamic railway stress on adjacent retaining structures, a laboratory investigation was conducted to study the effect of lateral dynamic pressure generation on steel walls. A test was carried out using a scale model that was 1/7th the size of the actual railway and steel sheet pile. These tests were performed under various parameters. The highest rate of increase in lateral stresses occurred during the initial loading cycles, and the dynamic lateral stress distribution was found to be non-linear. The most significant factor improving the performance of walls and railways is the increase in the soil's relative density, as it reduces active stresses and increases passive stresses. When the relative density of the sub-grade changes from 30% to 55% and from 55% to 75%, the active lateral stresses decrease by an average of 33.52% and 22.44%, respectively, while passive lateral stresses increase by 16.83% and 19.1%, respectively. Increasing the amplitude of dynamic loads imposed on the railway leads to an increase in the horizontal stresses generated on both the active and passive sides of the wall. Additionally, the horizontal distance between the wall and the railway inversely affects the dynamic lateral pressures.

Keywords: Dynamic stresses, Retaining wall, Railway, Sandy backfill.

INTRODUCTION

Retaining structures are essential in geotechnical engineering, as they keep earth masses back, reduce erosion and landslides, and protect adjacent structures (Constro, 2020). Most retaining walls are built for static loads, but railway sub-structures need sturdy barriers to protect the railway from dynamic stresses caused by train live loads (Yadav et al., 2018). Rail track design often incorporates retaining walls to reduce railway settlement, prevent collapses, and maintain safe working conditions (Nakajima et al., 2013). A single train may generate several wheel loads in seconds, rapidly and repetitively loading the soil in a cyclic manner (Xia et al. 2008). The railway superstructure ensures that wheel axial loads are distributed evenly throughout the sub-grade (Wang et al., 2021). By supporting sub-grade layers using retaining walls, settlement is reduced, extending the structure's lifespan and efficiency (Bilfinger 2013). Assessment of dynamic ground pressure is crucial to maintaining structural integrity (Salim, 2004). Although the lateral earth pressure and thrust location are frequently unknown and deviate from theoretical projections, wall displacement influences the wall pressure distribution under dynamic action (Ivanik, 2015). Adding weight to the grain sub-grade increases settlement buildup, earth pressure, and lateral movement in the soil (Sherif & Fang, 1994). The sub-structure has received less attention despite its significance and considerable impact on track maintenance costs, where sub-structure characteristics are more unexpected and harder to determine than super-structure (Selig & Waters, 1994). Living loads predominate, while dead loads are often over-shadowed by track foundation design principles (Burrow et al., 2007). Axle load is the basis for conventional design guidelines, while cyclic and dynamic loads behave differently from static loads (Dareeju, 2017). Dynamic deformations differ significantly from static loading conditions. Under dynamic loads, the retaining wall may settle and rotate differently (Chen et al., 2021), considering the impact of load cycles and the influence of wave propagation through the soil.

To clarify the effect of live loads generated during the passage of trains, a laboratory model was built to study the distribution pattern of lateral dynamic pressures on the sheet pile wall adjacent to the railway. The current study focuses on the distribution of dynamic lateral pressures at selected time instances, rather than on time histories at specific points. The device applied corrected sine wave loading, as proposed by Fattah et al. (2019), to simulate traffic loads.

EXPERIMENTS

Soil and Ballast Used

The sandy soil was dried and sieved on sieve no. 10 (2.0 mm), and then, the physical properties of the sand were determined per the standard specifications (USCS-ASTM), as shown in Table 1. The ballast is 1/7 of the original size. The size of ballast used in railways ranges from 20 mm to 65 mm with D_{60} = 46 mm, D_{30} = 34 mm & D_{10} = 27 mm (Gilani et al., 2022)) produced by breaking stones into smaller sizes. The ballast utilized is poorly graded according to (USCS-ASTM). Figure 1 shows the size distribution curves for sand and ballast used in this study.

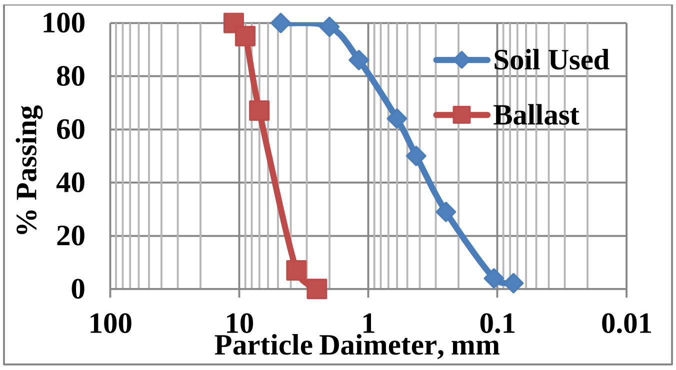

Figure 1. Ballast & sand grain size distribution curve

Table 1. Sand physical characteristics

Properties	Values
Specific gravity, (Gs)	2.66
D_{10}, mm	0.15
D_{30}, mm	0.26
D_{60}, mm	0.53
Coefficient of gradation, Cc	0.85
Coefficient of uniformity, Cu	3.53
Maximum dry unit weight, kN/m^3	18.0
Minimum dry unit weight, kN/m^3	15.2
Soil classification	SP
Minimum void ratio	0.48
Maximum void ratio	0.75

Model of Railway and Sheet Pile Wall

The scale used in the model is one-seventh of the actual dimensions of the railway (Gilani et al., 2022), where studies have been conducted on railway tracks in laboratory conditions at different scales; their range includes scales of (1:1) to (1:20). Modeled after the real railway in compliance with Iraqi regulations (Fattah et al., 2019), it features two steel rails of 65 cm in length and seven wooden sleepers, with each sleeper having a length (B) of (260) mm. The sheet pile wall has a thickness of (2) mm, a (600)-mm level, and a (600)-mm length to simulate the PZ40 (Das, 2011), where the wall height (H) is 200 mm. Figure 2a depicts the sheet pile wall utilized in the examination, while Figure (2b) shows the track.

Preparation of Lab Model

In a container of 1.6m × 0.75m × 0.75m with a front face of 15-mm thick plexiglas with three sides and a base of 5-mm thick steel, sand deposits are prepared using a modified vibrating compactor. In the beginning, the soil was placed at a height of 150 mm according to the specified density, forming a cushion under the wall to ensure that the container base does not affect the wall tip response, and then, the sheet pile wall was placed with the load cells (three for the active side and three for the passive side). The weight of the sand required to achieve the relative density was determined, since the unit weight and the volume of the sand are known. The total weight is divided into six equal weights, each one representing the weight required for a single layer, which has a thickness of (100) mm for the active and passive sides. The soil in each layer is compacted to the required depth. After completing the final layer, the top surface is scraped and leveled by a sharp-edged ruler to get a surface which is as close as possible to a flat surface. Following the same procedure for a single ballast layer (60-mm thickness), the railway was subsequently laid on top of the ballast and sloped down on either side at a ratio of around 1.25:1. Figure 2c illustrates the overall lab model. All of the sensors were brought into alignment by using dead weights ranging up to 5 kg, with a weight increase of 0.25 kg. The calibration equation has been obtained by drawing the pressure-reading relationship with the R^2 above 0.99 for all the sensors, as shown in Figure (3).

a. sheet pile wall

b. track

c. overall lab model & vibratory device

Figure 2. Physical models

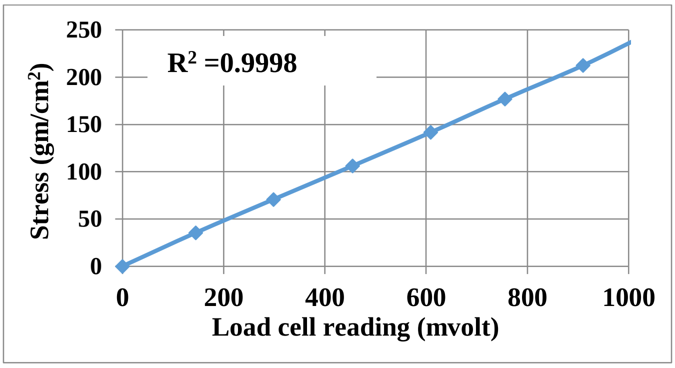

Figure 3. Calibration for load cell

The Setup of Loading

Figure 2c illustrates the impact of the vibratory device made at the University of Technology soil lab, which applied corrected sine wave loading to subject the models to live loading tests (Fattah et al., 2019). The device measures vertical settlement using a shaft encoder. The digital code from the shaft's movement is processed by an electro-mechanical device to determine settlement. A Programmable Logic Controller (PLC) is used to acquire data, record information, and identify settlements during testing, providing analysts instant access to valuable information. Also, it is used to pick a pre-determined test frequency, and this method analyzes data properly. The input and output data can be viewed on the LCD touchscreen panel of a PLC device using simplified ladder logic.

TEST RESULTS

81 model experiments were run at (2, 4, and 6) Hz up to 4000 loading cycles, which is within the usual frequency on the track, which is approximately up to 10.0 Hz for normal trains (Fattah et al., 2019). to examine the sheet pile wall's and railway's response. The experiments employed varying relative densities (Dr) of sand (30%, 55%, and 75%), where the values of internal friction angl were (ϕ) were (30.5, 35.5, and 39), respectively, dynamic load amplitudes were (2.2, 4.4, and 6.6 kN), and the distance between the sheet pile wall and the railway track (X) was equal to (1/2 H, 1/1 H, and 3/2 H).

Distribution Dynamic Lateral Stresses

Figure 4 illustrates samples of the distribution of dynamic lateral pressures generated along the height of the wall due to the dynamic surcharge from the railway. These pressures were recorded by pressure sensors (LC1 through LC3) for loose, medium, and dense soil as a function of depth for both the active and passive sides. The samples correspond to a dynamic load amplitude of 2.2 kN at a vibration frequency of 2 Hz and a distance ratio (X/H = 0.5). All curves show a non-linear lateral dynamic stress distribution for both the active and passive sides of the sheet pile wall in sub-grades under dynamic loading. Additionally, the values of lateral stresses are close to zero at the lower end of the wall, but increase significantly at the top, particularly in loose sand. The highest lateral stresses occur approximately at the middle of the wall on both the active and passive sides of the buried part. This conclusion is consistent with Grasso and Motta (2004).

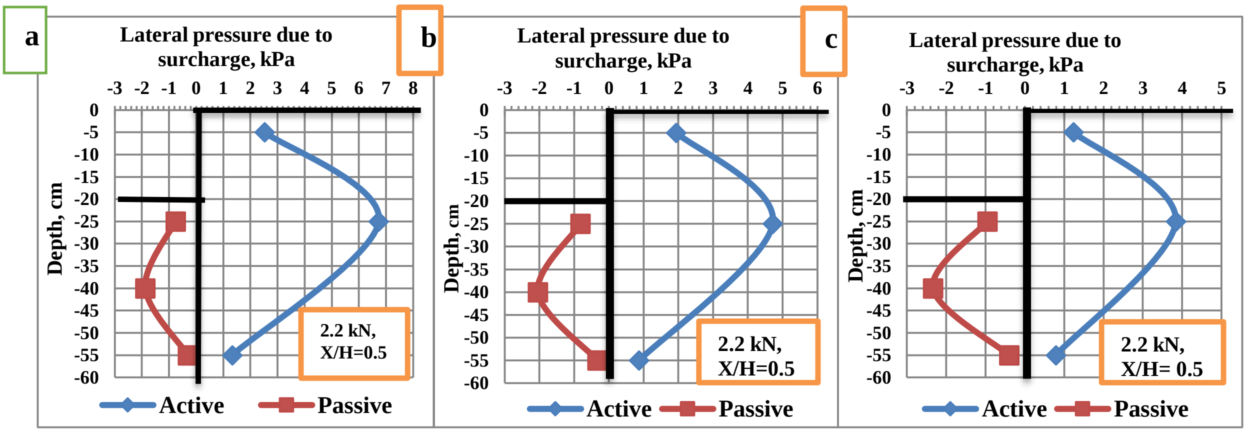

Figure 4. Distribution dynamic lateral pressures *versus* height of the wall under load amplitude 2.2 kN at 2-Hz frequency with (X/H= 0.5) in (a) loose, (b) medium and (c) dense sand

The Effect of Number of Loading Cycles

Figure 5 shows samples for the pattern of dynamic lateral pressures generated on the sheet wall, recorded by pressure sensors LC1 through LC3 for medium sand, as a function of the cycle loading for the active and passive sides of the wall. This figure corresponds to the dynamic load amplitude of (2.2) kN, the vibration frequency of (2) Hz, and (X/H= 0.5). All curves of these samples indicate that during the first 25 cycles of dynamic loading, there is a quick and sharp increase in lateral dynamic stresses on both the active and passive sides of the wall. Afterward, during the first 500 cycles, the stress values on the active side gradually begin to decline, while the values of the stresses on the passive side gradually begin to increase. Subsequently, the shape of the curves (both active and passive) stabilizes approximately horizontally in the remaining loading cycles, depending on the soil conditions and the test parameters. This behavior can be attributed to the fact that after the soil has been exposed to sufficient vibration, the densification process occurs. Anyhow, there is harmony between the lateral stress curves and the settlement and displacement curves of the rail and the wall. These results are in line with Asakerehl et al. (2012), who demonstrated that a limit value can be established for the buildup of stresses and that granular material will experience a decrease in the rate of permanent deformation with the continuance of repeated loading.

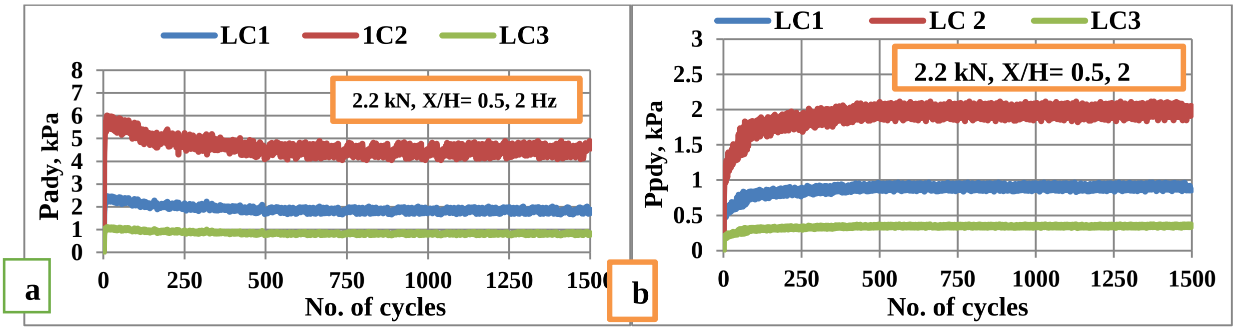

Figure 5. No. of cycles *versus* dynamic lateral stresses on the wall in medium sand under load amplitude (2.2) kN at 2-Hz frequency with (X/H) = 0.5: (a) active side & (b) passive side

Impact of Sub-grade Relative Density

To examine the impact of the relative density of the backfill on the lateral dynamic stresses generated on the sheet wall under various dynamic loading conditions with 2-Hz frequency vibration and (X/H= 0.5) resting on loose, medium, and dense sand. Figure (6) illustrates the findings. Increasing the relative density of the soil results in a decrease in the dynamic lateral pressures on the active side and an increase on the passive side of the wall. When the relative density of sub-grade increases from 30% to 55% and from 55% to 75%, the active lateral stresses fall on average by roughly 33.52% and 22.44%, while the average increases in cumulative passive lateral stresses are roughly 16.83% and 19.1%, respectively. It is evident that as the soil density increases, the angle of internal friction (ϕ) also increases, causing the failure wedge line to move farther away from the center of the live loads imposed on the track. As a result, the lateral stresses generated on the active side decrease while those on the passive side increase. These results are consistent with the findings of Mahdi et al. (2021), who showed that an increase in the angle of internal friction (ϕ) leads to a decrease in active earth pressure.

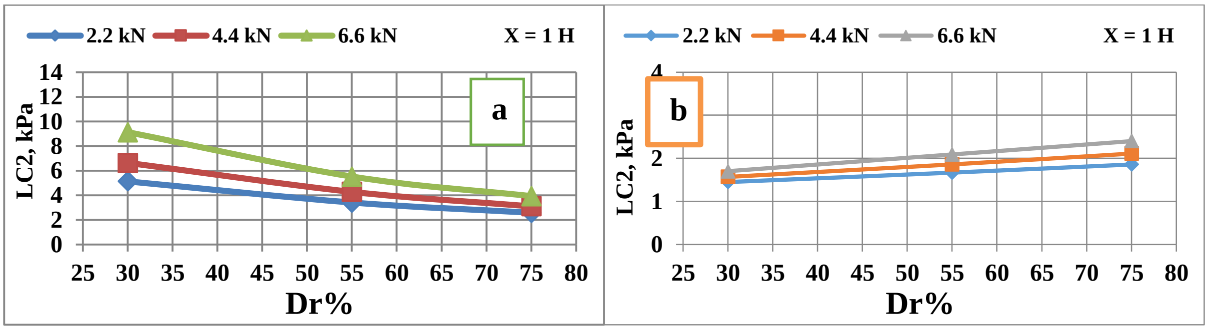

Figure 6. Cumulative dynamic lateral stress in active side (a) and passive side (b) of wall *versus* sub-grade relative density at 2-Hz frequency with different dynamic loads and (X/H = 1)

Dynamic Load Amplitude's Influence

The outcomes of tests on loose, medium, and dense sand at a frequency of 2 Hz for different load amplitudes and (X/H= 1.5) are shown in Figure 7. According to this figure, when dynamic load amplitudes rise, the dynamic lateral stress on both the active and passive sides of the wall increases. The dynamic lateral stress for the active and passive sides increases by approximately (30.15%), (6.22%) and (37.48%), (10.87%) for loose soil, (24.9%), (10.67%) and (29.4%), (13.48%) for medium soil, and (22.12%), (11%), and (24.97%), (14.8%) for dense soil, respectively, as a result of the change in the dynamic load amplitude from (2.2 kN) to (4.4 kN) and from (4.4 kN) to (6.6 kN). The dynamic load used in the lab model (2.2) kN simulated the train's axel live load according to (GTS, 2004), while the mimic load (2.2) kN was doubled to (4.4 and 6.6) kN to know the effect of increasing live load on the railway system's performance. This can be attributed to the widening of the circumference of the bulb of stress generated under the railway with the increase in the live loads imposed on it.

This result is consistent with Aswad et al. (2023), who examined the lateral earth pressure distribution on a gravity retaining wall.

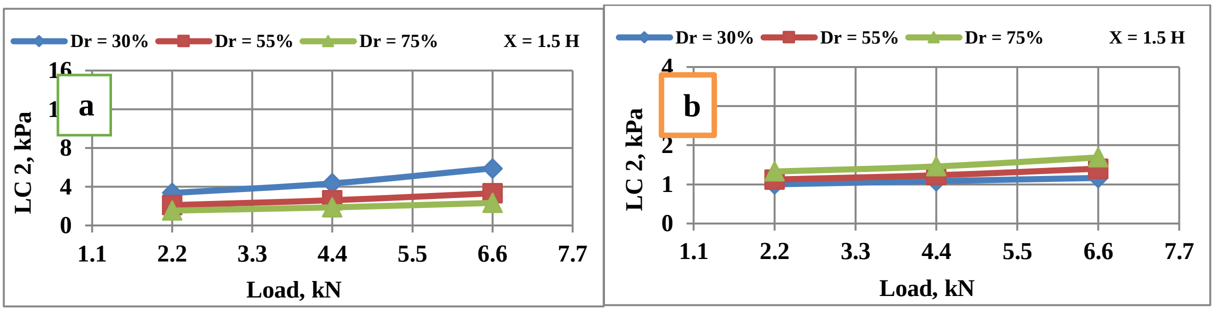

Figure 7. Cumulative dynamic lateral stress in active side (a) and passive side (b) of wall *versus* dynamic load with 2-Hz frequency in different sub-grade relative density values with (X/H = 1.5)

Railway Location's Impact from Sheet Pile Wall

Figure 8 illustrates the relationship between the dynamic lateral stresses on the sheet pile wall and the horizontal distance (X) to examine the impact of the railway's location on the wall in dense sand under different load amplitudes. It is evident that as the horizontal distance ratio (X/H) increases, the cumulative dynamic lateral stresses on both the active and passive sides of the wall decrease. Specifically, moving the railway from 0.5H to 1H and then from 1H to 1.5H reduces the active dynamic lateral stress by approximately 28.81% and 37.73%, while the passive dynamic lateral stresses decrease by 23.54% and 30.23%, respectively. The larger reduction in active lateral pressure, compared to passive lateral pressure on the wall, can be attributed to the fact that increasing the horizontal distance between the wall and the railway reduces the impact of the cyclic load on the wall, as the load is dispersed and moves away from the failure wedge zone on the active side of the soil (Naji et al., 2023).

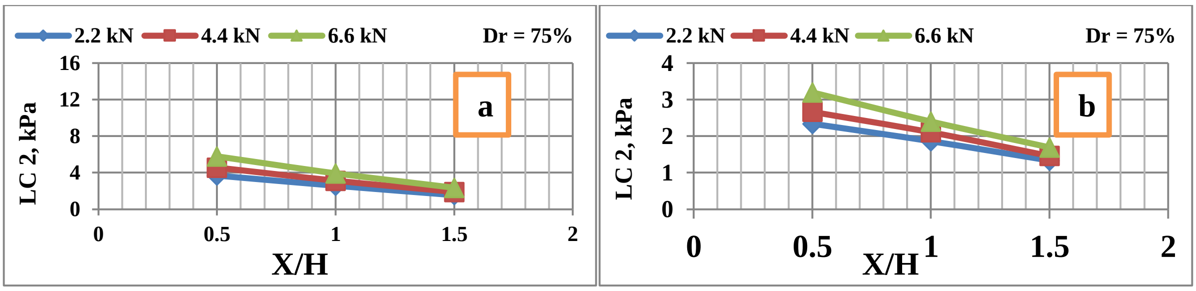

Figure 8. Cumulative dynamic lateral stress in active side (a) and passive side (b) of wall *versus* (X/H) for different dynamic loads at 2-Hz frequency with Dr = 75%

Wall Movement Pattern

The pattern in which the wall moves in loose, medium, and dense sandy soil when subjected to the loads created by the railway is evident in Figure (9). In loose soil, the wall tends to slide and spin around its bottom, but in dense and medium soil, it rotates around its bottom only.

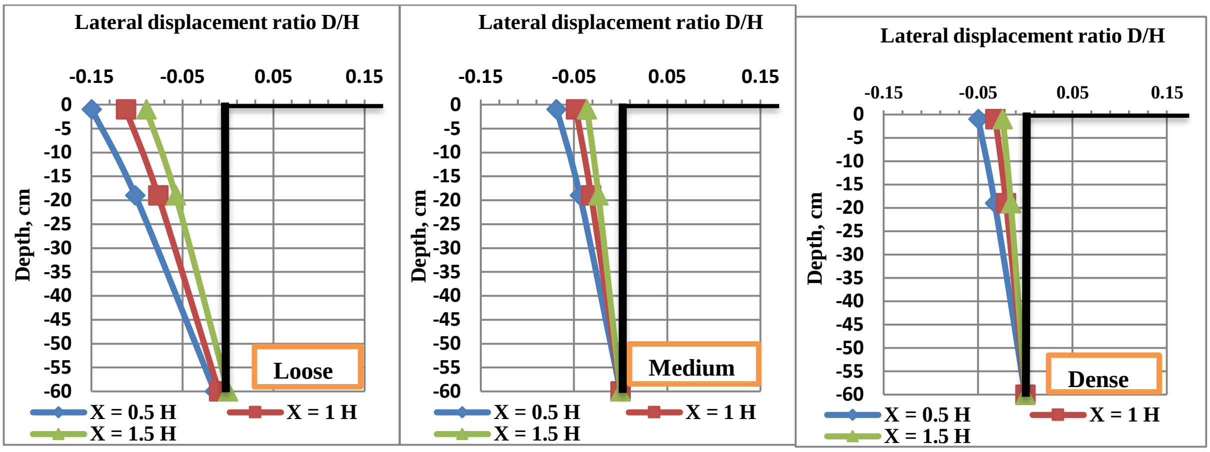

Figure 9. Wall height *versus* lateral wall displacement ratio (D/H) at various sensor positions on the wall under dynamic load 6.6 kN at 2 Hz

Railway Settlement and Lateral Wall Dynamic Stresses

When the cyclic number *versus* settlement ratio (S/B) curves in Figure 10 are compared to the cyclic number *versus* lateral dynamic stress curves in Figure (5), it was found that there is a direct relationship between railway settlement and active dynamic lateral stresses. Do et al. (2024) demonstrated that the cumulative stress and strain are directly impacted by the cyclic loading amplitude.

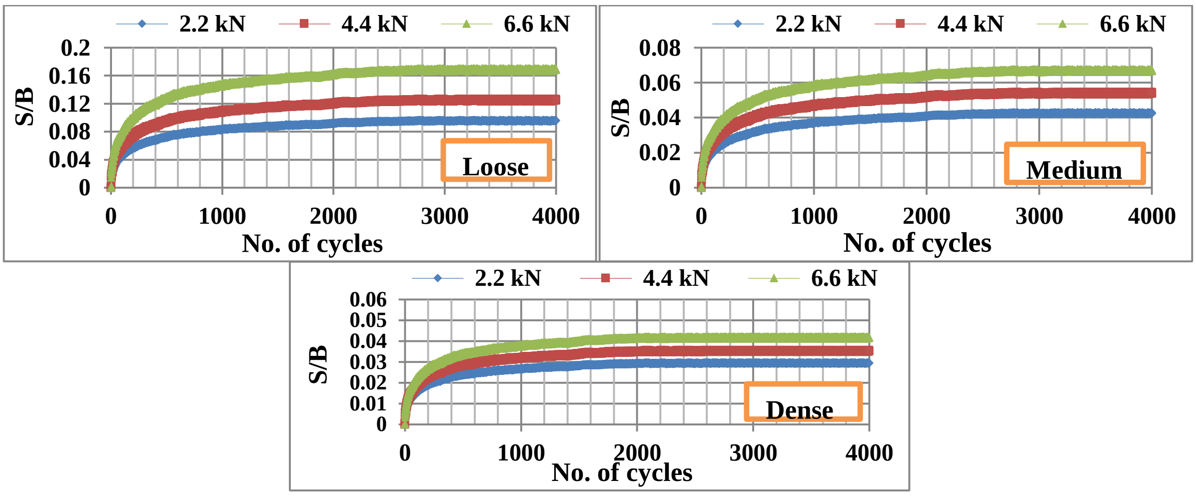

Figure 10. Cyclic number *versus* settlement ratio (S/B) at a frequency of 2 Hz, with varying load amplitudes for (X) = 0.5 H

CONCLUSIONS

1. During the first 25 to 50 dynamic loading cycles, there is a sudden increase in the wall's active and passive lateral dynamic stresses. Then, over the next 500 cycles, active stress levels decrease, but passive stress levels increase. Depending on the soil type and test conditions, the active and passive curves stabilize almost horizontally in the remaining loading cycles.
2. There is a non-linear relationship between the total number of loading cycles and cumulative dynamic lateral stress. The distribution of dynamic lateral stresses, both active and passive, throughout the wall's depth that supports loose, medium, and dense sand under train live loading, is non-linear.
3. As the relative density of the backfill soil increases, the lateral active dynamic pressure exerted on the sheet pile wall decreases while the lateral passive dynamic pressure that supports the wall increases. Consequently, the track settling and lateral displacement of the wall decreased, leading to an

improvement in the overall performance of the railway system.

4. As the amplitude of vertical dynamic loads increased, the active and passive sides of the sheet pile wall experienced an increase in dynamic lateral stress. However, the active side is much more affected by increased dynamic loads than the passive side.
5. Increasing the distance between the railway and the sheet pile wall lowers the values of cumulative dynamic lateral stress on both the active and passive sides, when all other parameters are kept constant.
6. The sheet pile walls slides and revolves around its bottom in loose soil, while it only revolves around its bottom in medium and dense soils. The sheet wall's dynamic horizontal displacement had its maximum value at the top under all circumstances.
7. Finally, to improve wall design in railway environments and minimize the effects of cyclic loading, the backfill’s relative density should exceed 75%, and the horizontal distance between the track and the wall should be greater than 1.5H within the permissible live load.

REFERENCES

Asakerehl, A., Tafreshi, S.N.M., & Ghazavi, M. (2012). Strip footing behavior on reinforced sand with void subjected to repeated loading. *International Journal of Civil Engineering, 10*, 140-152.

Aswad, M.F., Fattah, M.Y., & Reham, E.H. (2023). Lateral stresses on retaining wall supporting sandy soil under dynamic footing loads. *Geotechnical and Geological Engineering*. https://doi.org/10.1007/s10706-023-02542-1

Bilfinger, W. (2013). General report of TC 207 foundations and retaining structures. In: *Proceedings of the 18th International Conference on Soil Mechanics and Geotechnical Engineering (ICSMGE)* (pp. 1915-1922). Paris, France.

Burrow, M.P.N., Bowness, D., & Ghataora, G.S. (2007). A comparison of railway track foundation design methods. *Proceedings of the Institution of Mechanical Engineers, Part F: Journal of Rail and Rapid Transit, 221*(1), 1-12.

Chen, C., Chang, L., & Loh, C. (2021). A review of spectral analysis for low-frequency transient vibrations. *Journal of Low Frequency Noise, Vibration and Active Control, 40*, 656-671.

Constro Facilitator. (2020). *Retaining wall design and its types used in construction.* https://constrofacilitator.com/retaining-wall-design-and-its-types-used-on-construction/. Accessed on: Dec. 5, 2024.

Dareeju, B.S. (2017). *Performance evaluation of unsaturated rail track foundations under cyclic moving wheel load.* PhD Thesis. Queensland University of Technology, Brisbane, Australia.

Das, B. (2011). *Principles of foundation engineering*. D.B.M. Contractors.

Do, V.T., Nguyen, V.H., & Pham, D.T. (2024). Behavior of sand specimens subjected to cyclic loads under drained and undrained conditions in variable loading amplitudes. *Jordan Journal of Civil Engineering, 18*(2). https://doi.org/10.14525/JJCE.v18i2.09

Fattah, M.Y., Mahmood, M.R., & Aswad, M.F. (2019). Stress distribution of railway track over geogrid-reinforced ballast underlain by clay. *Earthquake Engineering and Engineering Vibration, 18*, 77-93. https://doi.org/10.1007/s11803-019-0491-z

Gilani, V.N.M., Habibzadeh, M., Hosseinian, S.M., & Salehfard, R. (2022). A review of railway track laboratory tests with various scales for better decision-making about more efficient apparatus using TOPSIS analysis. *Advances in Civil Engineering*. https://doi.org/10.1155/2022/9374808

GTS-Guidelines for Temporary Shoring. (2004). Burlington North Santa Fe Railway and Union Pacific.

Ivanik, O. (2015). Principles and methods of the regional landslide hazard assessment based on analysis of the rock mass stress-strain state. In: *14th EAGE International Conference on Geoinformatics*. European Association of Geoscientists & Engineers. https://doi.org/10.3997/2214-4609.201412393

Lo Grasso, A.S., Maugeri, M., & Motta, E. (2004). Experimental results on earth pressures on rigid walls under seismic conditions. In: *13th World Conference on Earthquake Engineering* (Paper No. 1808). Vancouver, BC, Canada.

Mahdi, T.K., Al-Neami, M.A., & Rahil, F.H. (2021). An experimental study on laterally loaded winged pile in sandy soil. *IOP Conference Series: Earth and Environmental Science, 856*(1). https://doi.org/10.1088/1755-1315/856/1/012051

Naji, K.N., & Al-Neami, M.R.M. (2023). The impact of generated loading from train passing on the dynamic response of retaining walls: A review. *AIP Conference Proceedings, 3219*(1). https://doi.org/10.1063/ 5.0237076

Nakajima, S., Shinoda, V., & Abe, K. (2013). Inspection of structural health of existing railway retaining walls. In: *18th International Conference on Soil Mechanics and Geotechnical Engineering (ICSMGE)* (pp. 2059-2062). Paris, France.

Salim, M.W. (2004). *Deformation and degradation aspects of ballast and constitutive modelling under cyclic loading.* PhD Thesis. University of Wollongong, Wollongong, NSW, Australia.

Selig, E.T., & Waters, J.M. (1994). *Track geotechnology and sub-structure management*. Thomas Telford.

Sherif, M.A., & Fang, Y.S. (1994). Dynamic earth pressures on walls rotating about top. *Soils and Foundations, 24*(4), 109-117.

Wang, T., Luo, Q., Zhang, L., Xiao, S., & Fu, H. (2021). Dynamic response of stabilized cinder sub-grade during train passage. *Construction and Building Materials, 270*, 121370. https://doi.org/10.1016/j.conbuildmat.2020.121370

Xia, F., Cole, C., & Wolfs, P. (2008). The dynamic wheel-rail contact stresses for wagon on various tracks. In: *Proceedings of the 8th International Heavy Haul Conference* (Vol. 265, pp. 1549-1555).

Yadav, P.A., Padade, A.H., Dahale, P.P., & Meshram, V.M. (2018). Analytical and experimental analysis of retaining wall in static and seismic conditions: A review. *International Journal of Civil Engineering and Technology, 9*(2), 522-530.